Superhydrophobic nanostructured ZnO thin films on aluminum alloy substrates by electrophoretic deposition process

Ying Huang, D. K. Sarkar*, X-Grant Chen

Centre Universitaire de Recherche sur l'Aluminium (CURAL),

Université du Québec à Chicoutimi, 555 Boulevard de l'Université,

Chicoutimi,Québec, Canada, G7H 2B1

ABSTRACT

Superhydrophobic thin films have been fabricated on aluminum alloy substrates by electrophoretic deposition (EPD) process using stearic acid (SA) functionalized zinc oxide (ZnO) nanoparticles suspension in alcohols at varying bath temperatures. The deposited thin films have been characterized using both X-ray diffraction (XRD) and infrared (IR) spectroscopy and it is found that the films contain low surface energy zinc stearate and ZnO nanoparticles. It is also observed that the atomic percentage of Zn and O, roughness and water contact angle of the thin films increase with the increase of the deposited bath temperature. Furthermore, the thin film deposited at 50 °C, the films

* Corresponding author: D. K. Sarkar

University Research Center on Aluminum (CURAL),

University of Québec at Chicoutimi,

555, Boulevard de l'Université, Chicoutimi (QC), Canada G7H 2B1

Tel.: 1-418-545 5011 ext. 2543

E-mail: dsarkar@uqac.ca

1. Introduction

A surface that provides non-wetting characteristics with water contact angle higher than 150° is termed as a superhydrophobic surface. After the discovery of superhydrophobic surfaces in nature [1, 2], many artificial superhydrophobic coatings have been fabricated by mimicking nature [3, 4]. In order to create superhydrophobic surfaces, it is observed that creation of a certain micro-nanoroughness structures promotes the entrapment of the air in the space between the rough features. In addition, lowering the surface energy helps to reduce the affinity of water drops with a surface thereby weakening the water-surface interaction.

Zinc oxide (ZnO) is widely use in solar cells [5], gas sensors [6], transistors [7], ultraviolet lasers [8], UV detectors [9] etc. Superhydrophobic ZnO thin films have been successfully synthesized by many synthetic routes, e.g., physical vapor deposition [10], chemical bath deposition (CBD) [11], electrodeposition [12, 13], etc [14-16]. The literatures show ZnO thin films can be superhydrophobic without any low surface energy passivation layers [10, 14, 15]. However, most of the cases an extra layer was incorporated to reduce the surface energy of ZnO to obtain superhydrophobic properties [12, 13, 16].

Electrophoretic deposition (EPD) is a wet-deposition process in which colloidal charged particles suspended in a liquid medium migrate under the influence of an electric field and get deposited on the surface of the electrode. When a sufficient electric field is applied to a colloidal suspension, they get deposited on the oppositely charged electrodes [17, 18]. A review on the fundamentals and applications of electrophoretic deposition (EPD) describes the effects of time, applied potential, concentration of solid in suspension, etc., [18]. Recently, EPD process has been used to prepare superhydrophobic surfaces by fabricating rough structures with low surface energy

materials. Joung and Buie fabricated superhydrophobic surfaces using electrophoretic deposition (EPD) of hydrophobic SiO_2 particle suspension modified by polydimethylsiloxane (PDMS) at room temperature [19]. Ogihara *et al*. prepared superhydrophobic SiO_2 particle/silicone resin composite coatings by EPD at room temperature [20]. They have also fabricated superhydrophobic colored films by EPD of hydrophobic pigment particles on substrates [21]. However, the effect of bath temperature on the EPD process to prepare thin films as well as fabricate superhydrophobic surfaces is not found in the literatures. Recently, we have used electrochemical modification and electrodeposition techniques to prepare superhydrophobic copper and aluminum alloy substrates [3, 4, 22]. In the present study, we develop the one-step electrophoretic deposition (EPD) process to fabricate superhydrophobic ZnO thin films on aluminum alloy substrates using stearic acid (SA)-functionalized ZnO nanoparticles suspension. The effects of the bath temperatures on the characteristics of deposited ZnO thin films and its superhydrophobic properties have been studied.

2. Experiments

In electrophoretic deposition process to prepare superhydrophobic ZnO thin films on aluminum alloy substrates, as-purchased hydrophilic ZnO particles (average particle diameter of 30 nm from MKNano, Ontario, Canada) were added in a mixture of 0.01 M ethanolic stearic acid (SA), 2-propanol and tert-butyl alcohol (vol. = 1:2:4) [23], followed by ultrasonication for one hour. In the case of preparing non-functionalized ZnO thin films on aluminum alloy substrates, ethanol, 2-proponal and tert-butyl alcohol mixed solution with the same ratio was applied. Though the concentration of nanoparticles were varied from 0.14 g/L to 1.4 g/L, the results of 1.4 g/L were only given in this manuscript. As-rolled aluminum alloy sheets, having rolled lines, have been used as

aluminum alloy substrates for more efficient in economical and time-saving point of view instead of using polished aluminum alloy substrates. A pair of cleaned AA6061 aluminum alloy substrates was vertically immersed in the suspension and kept at a distance of 1.5 cm and a 30 V DC was applied for 10 minutes at the bath temperature ranging from 10-50 °C. The bath temperature was controlled using a thermal bath normally used for cooling the solution for anodization of aluminum alloy substrates. The morphological and elemental analyses were performed using a scanning electron microscope (SEM, JEOL JSM 6480 LV) equipped with energy dispersive x-ray spectrometer (EDX). A thin gold layer was sputtered on the modified surfaces with Polaron sputter coater (SC7640) for improving the resolution of non-conducting samples during SEM and EDX studies. The chemical composition of surfaces was analyzed by X-ray diffraction (XRD, D8 discover with Cu K_{α} wavelength 0.154 nm) and infrared reflection absorption spectroscopy (IRRAS, Nicolet 6700FT-IR). As-purchased and SA-functionalized ZnO nanoparticles were analyzed by making pellets with KBr powder and using Fourier Transform Infrared (FTIR, Perkins Elmer Spectrum One) spectroscopy. The roughness of surfaces was measured using an optical profilometer (MicroXAM-100 HR 3D surface profilometer). The wetting characteristics of the sample surfaces were carried out by measuring static contact angles (abbreviated as CA) using a First Ten Angstrom contact angle goniometer. Furthermore, the dynamic contact angle (abbreviated as CAH) of the superhydrophobic surface was also measured by holding the water drop with a stationary needle in contact with the superhydrophobic surface and moving the goniometer stage in one direction. CAH is defined as the difference between the advancing and receding contact angle as published before [3, 4, 24].

3. Results and discussion

Fig. 1(a) shows the x-ray diffraction (XRD) patterns of (aI) as-received AA6061 aluminum alloy substrate, and (aII) thin film of SA-functionalized ZnO electrophoretically deposited at bath temperature of 50 °C on the AA6061 aluminum alloy substrate in the 2θ scan range of 30-70°. The XRD pattern (aII) shows the characteristic peaks of ZnO (100), (002), (101) and (110) at 31.82°, 34.47°, 36.19° and 56.78°, respectively [25], confirming the ZnO deposition on Al alloy substrate. It also shows the peaks at 38.47°, 44.72° and 65.1°, respectively, which are in good agreement with the characteristic peaks of Al (111), (200) and (220) in as-received Al alloy substrate pattern (aI) [26]. The crystal size of the deposited ZnO at 50 °C bath temperature was calculated by the Debye-Scherrer's formula with the help of full width at half maximum (FWHM) of the XRD peak.:

$$D = \frac{0.9\,\lambda}{\beta \cos\theta} \quad (1)$$

Where λ is the wavelength (0.154 nm) and β is full width in radian at half maximum of the peak and θ is the Bragg's angle of the XRD peak. The crystallite size of ZnO deposited on aluminum alloy substrate at 50 °C is calculated to be 26 nm, which is consistent with the average diameter of 30 nm of as purchased ZnO nanoparticles.

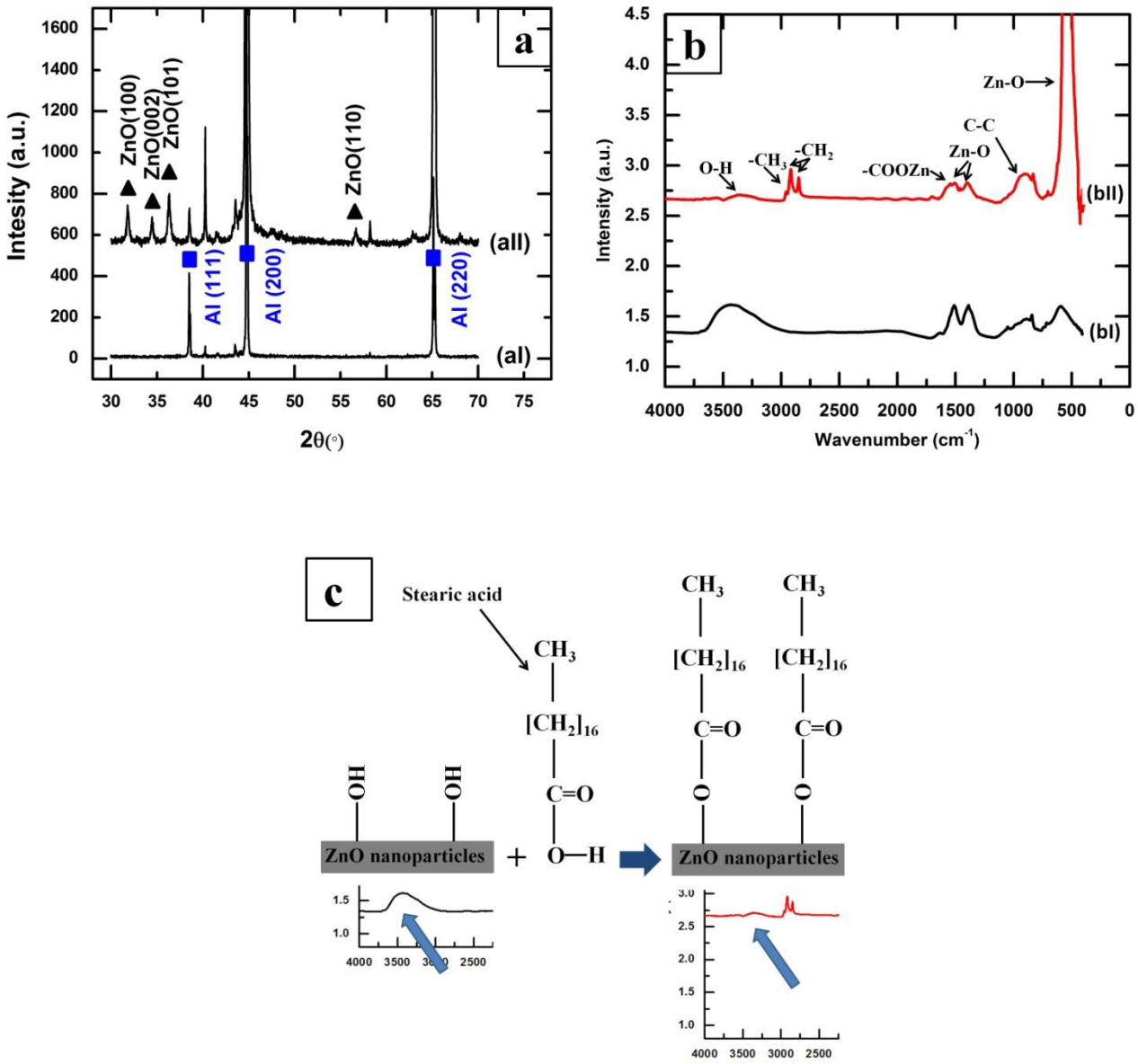

Figure 1 (a) XRD patterns of (aI) aluminum alloy substrate and (aII) electrophoretic deposited SA-functionalized ZnO thin film on the aluminum alloy substrate; (b) FTIR spectrum of (bI) the palette of as-received ZnO nanoparticles with KBr powder and (bII) IRRAS spectrum of SA-functionalized ZnO film on aluminum alloy substrate; (c) The schematic graph of interaction between SA and ZnO.

Fourier Transform Infrared spectroscope (FTIR) and Infrared reflection absorption spectroscopy (IRRAS) were used to analyze the atomic bonding in (bI) ZnO nanoparticles and (bII)

the SA-functionalized ZnO thin film on aluminum alloy substrate in Fig. 1(b), respectively. ZnO nanoparticles were analyzed by FTIR as powder pellets with KBr. The bands centered at 1506 cm^{-1} and 1400 cm^{-1} were observed both in the IRRAS spectrum ((bII)) as well as FTIR spectra ((bI)) are due to the ZnO [27]. Furthermore, the peak at 560 cm^{-1} also comes from ZnO stretching mode. The observation of ZnO peaks is consistent with that of XRD pattern of SA-functionalized ZnO electrophoretically deposited alloy in Fig. 1(a). The peaks at 2850 cm^{-1}, 2919 cm^{-1} and 2962 cm^{-1}, which appeared in the spectrum of SA-functionalized ZnO thin film on alloy surface rather than ZnO spectrum, are from $–CH_2$ and $-CH_3$ vibrations as shown in (bII). The appearance of these bands confirm the presence of low surface energy components of methylated in the coatings [28]. It is to be mentioned that, a low intense new peak at 1550 cm^{-1} is due to the -COOZn bonds appeared in the spectra of SA-functionalized ZnO thin film surface [13]. The infrared studies confirm the formation of zinc stearate hence the functionalization of zinc oxides by stearic acid and their thin film formation by EPD process as presented in the Fig. 1(b). IRRAS was used to evaluate the thin films on the aluminum alloy substrates as IR does not pass through metals. The overall objectives were to evaluate both the as-received ZnO nanoparticles and as well as the thin films on aluminum alloy substrates. However, the intensity of the peaks can't be compared between these two different analyzing methods. Fig. 1(c) shows the schematic presentation of the interaction between SA and ZnO. It shows that the ZnO surface was functionalized by SA molecules, with the formation of zinc stearate. The –OH bonding on ZnO surface was replaced by –COOZn in the interaction between ZnO and SA, which explained the disappearance of –OH after ZnO functionalized by SA molecules in Fig. 1(b).

Table 1 summarizes the properties of SA-functionalized ZnO thin films deposited by EPD

process at varying bath temperatures. Fig. 2(a) shows the SEM image of the surface of as-received Al alloy substrate, which has a surface roughness of 0.45 μm and water contact angle of 87 ± 3° (inset of the Figure). Anyone must be aware that rolled sheets generally shows the rolled lines on its surfaces and therefore, will have a certain roughness inherently. Fig. 2(b) shows the thin films of SA-functionalized ZnO deposited at the bath temperature of 10 °C. It is clear from the Figure that the formation a few white microdots on the aluminum alloy substrate. Interestingly the contact angle of water on this surface is increased to 101 ± 4° while the surface roughness remaining almost the same as untreated aluminum alloys substrate (0.48 μm). This increase of water contact angle is due to the presence of SA-functionalized ZnO, as stearic acid (SA) reduces the surface energy due to the presence of $-CH_2$ and $-CH_3$ radicals. Furthermore, the number density of microdots increases slightly with the increase bath temperature of 20 °C from 10 °C as shown in Fig. 2(c). Evidently, a slight increase of surface roughness from 0.48 μm to 0.64 μm is observed. It has been observed that the contact angle also increases from 101 ± 4° to 114 ± 4° due to the increase of roughness of the thin films associated with the increase of the bath temperatures. Moreover, increasing bath temperatures to 30 °C and 40 °C lead to the more amounts of deposits and higher coverage of SA-functionalized ZnO microdots on the aluminum alloy substrates as evident from Fig. 2(d) and (e). The roughness and the water contact angle of the films deposited at 30 °C and 40 °C are 0.81 μm and 127 ± 2° and 2.72 μm and 139 ± 2°, respectively. The similar microdots structure formations were also reported in the literatures [29-31]. A thin film with complete coverage is observed when the bath temperature is increased to 50 °C as shown in Fig. 2(f). The higher magnification micronanostructure is shown in the inset of Fig. 2(f). The morphology of the SA-functionalized ZnO thin films deposited at bath temperature of 50 °C is similar to the

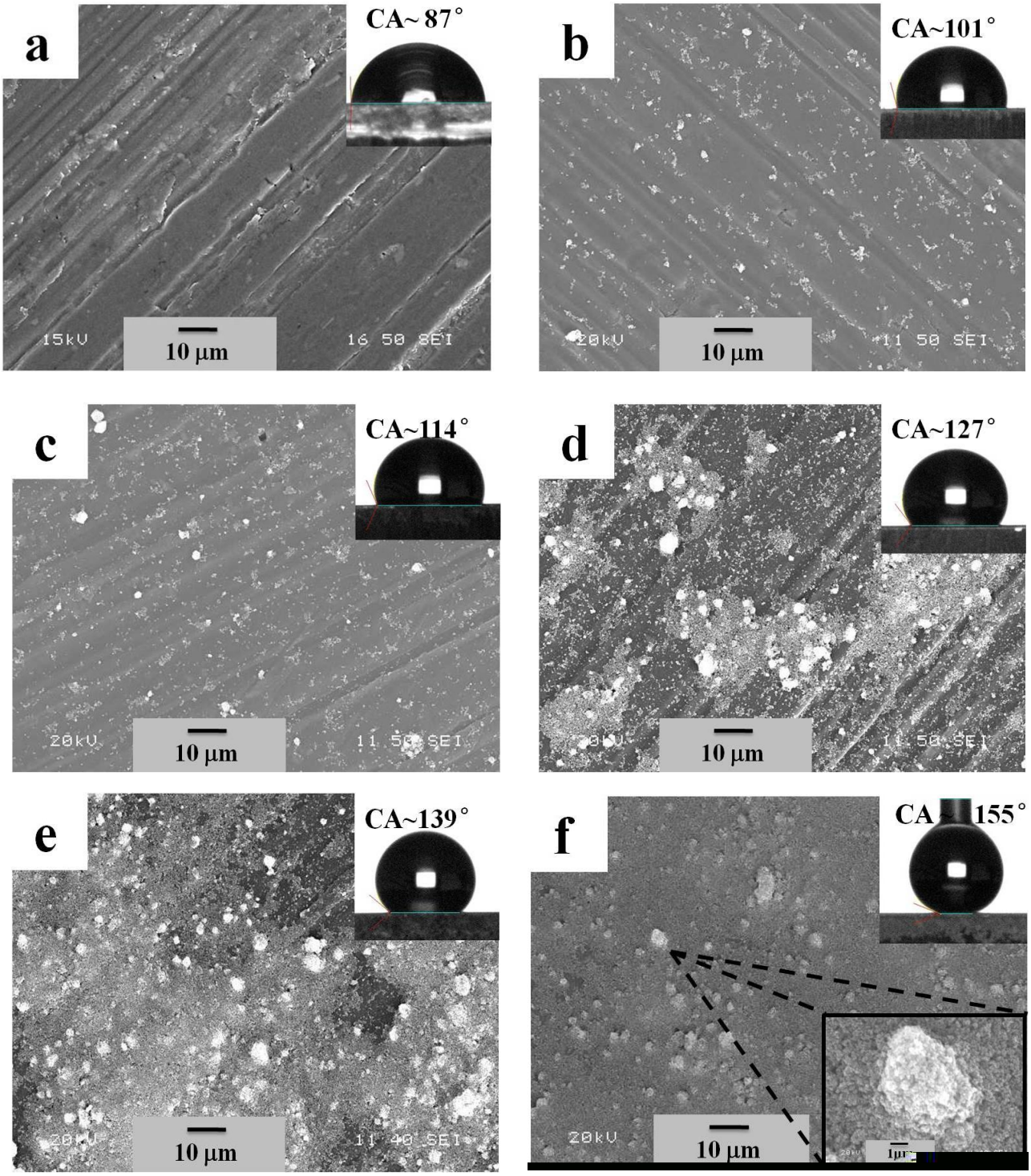

Figure 2 SEM images of (a) the surface of as-received Al alloy substrate; (b-f) the SA-functionalized ZnO thin film on Al alloy substrates at bath temperature of EPD process (b) 10 °C, (c) 20 °C, (d) 30 °C, (e) 40 °C and (f) 50 °C. The insets of SEM images show the images of water drop on respective surfaces. Also, the inset of

down-right-corner of (f) shows the magnified image of a cluster.

morphology of the flower-like micro-nanostructures on the superhydrophobic copper surfaces in our previous study by electrochemical modification using ethanolic stearic acid [3], which is comparable to that of the lotus leaves morphology [32]. The combination of micro-nanorough clusters of ZnO nanoparticles with the low-surface-energy stearic acid molecules transforms the aluminum alloy substrates to superhydrophobic. The films deposited at 50 °C have a surface roughness of 4.54 μm providing a high contact angle of 155 ± 3°, as shown in the inset of Fig. 2(f), as well as a contact angle hysteresis of 5 ± 2°. Stearic acid (SA) passivated flat ZnO surface prepared by sol-gel process shows a CA of 60° (see the supplementary material). Therefore, the thin films prepared by SA-functionalized ZnO nanoparticles follow the Cassie-Baxter model [33].

The thin films were prepared using as-received ZnO nanoparticles to compare the wetting properties with the thin films prepared with the SA-functionalized ZnO nanoparticles. The morphologies of the thin films prepared by EPD process using as-received (in other words non-functionalized) ZnO nanoparticles are shown in Fig. 3. The morphologies are very similar as found for the thin films prepared from the SA-functionalized ZnO nanoparticles. The wetting properties of these films are presented in the inset of the images as well as the down graph of Fig. 4(b). It is found that the CA of the films reduces with the increase of the bath temperature that might be due to the increase of roughness of the films associated with the size of the cluster [34]. The contact angle is found be as low as 9° when the film was deposited at 50 °C bath temperature.

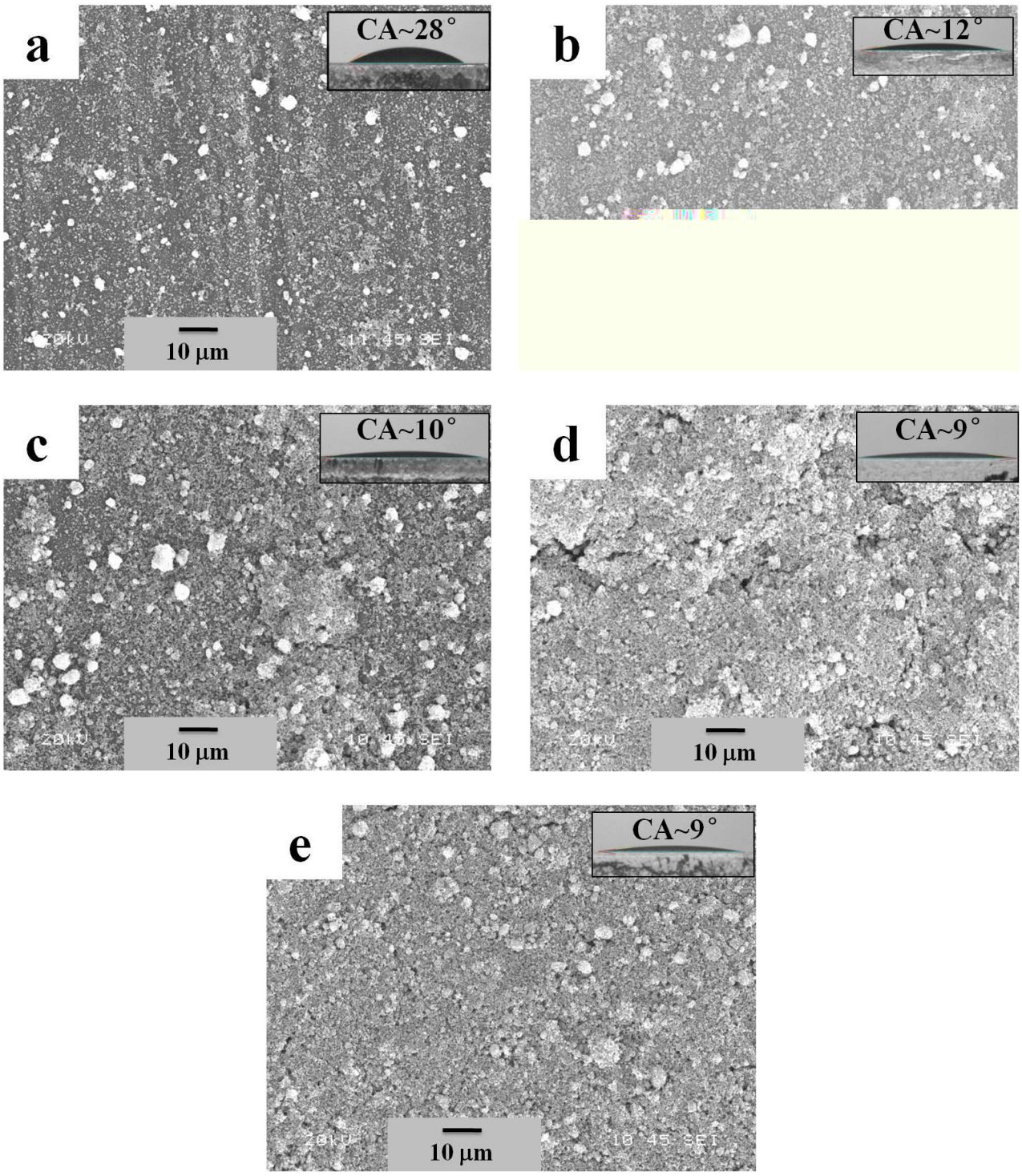

Figure 3 SEM images showing the morphologies of the thin films prepared by EPD process using as-received (in other words non-functionalized) ZnO nanoparticles: (a) 10 °C, (b) 20 °C, (c) 30 °C, (d) 40 °C and (e) 50 °C. The insets of SEM images show the images of water drop on respective surfaces.

The reduction of the contact angle (CA) due to the wetting of the surface according to the Wenzel model [35] as a smooth ZnO thin films gives a water contact angle of 27° prepared by sol-gel process (see the supplementary material). However, it has been reported that some cases the ZnO thin films can be superhydrophobic without any passivation [10, 14, 15] but most of the cases a layer of low surface energy films or monolayers were used to obtain superhydrophobic properties [12, 13, 16] as in our case. Compared with the morphologies of petal, tube or wire structures, as reported in the literatures [36, 37] spherical cluster of SA-functionalized ZnO particles observed in the present studies. The formation of spherical cluster is more probable as it requires minimum Gibbs free energy barrier to form as compared to other forms like, cube, petal or wire. As reported by Laurenti [10], ZnO nanowires were grown by hydrothermal method on ZnO seed layer. However, in our case, ZnO nanoparticles (either as-received or SA-functionalized) were deposited on the aluminum alloy substrates (possible having a native oxide layer) by EPD process. Due to the dissimilar properties of the substrate and deposited materials, their surface energies are not the same; the expected growth mode would be Volmer-Weber (island growth). Evidently, we have observed the formation of islands of ZnO or SA-functionalized ZnO on aluminum alloy substrates. Recently, our group has shown that superhydrophobic ZnO thin films can be deposited by chemical bath deposition process. The SA-functionalized ZnO thin films were produced by the reaction between $Zn(NO_3)_2$, NH_4OH and stearic acid in an ethanolic solution driven by thermal energy. However, in the present study we have used as-purchased 30 nm hydrophilic ZnO nanoparticles and chemically modified them by SA and used EPD process to prepare superhydrophobic thin films driven by electrical energy.

Table I Properties of SA-functionalized ZnO thin films deposited by EPD process at varying bath temperatures.

Bath temperature	Atomic percentage of Zn (%) by EDX	Surface roughness (μm)	Contact angle (°)	Intensity of XRD peak of ZnO (101) plan (a.u.)
As-received Al alloy substrate	Not applicable	0.45 ± 0.03	87 ± 3	0
10 °C	Non detected	0.48 ± 0.02	101 ± 4	17 ± 0.4
20 °C	Non detected	0.64 ± 0.09	114 ± 2	17 ± 0.7
30 °C	4	0.81 ± 0.10	127 ± 2	18 ± 0.9
40 °C	25	2.72 ± 0.17	139 ± 2	30 ± 1.0
50 °C	70	4.54 ± 0.23	155 ± 3	65 ± 4.5

Fig. 4 shows the variation of surface roughness and water contact angle of the films of SA-functionalized ZnO nanoparticles prepared with the increase of bath temperatures. It is found that the surface roughness increases with the increase of bath temperature and have a sudden jump at 40 and 50 °C (Fig. 4(a)). The increase of roughness with the increase of deposition temperature may be due to the increase size and density of the micro-clusters of ZnO as seen in the SEM. On the other hand the contact angle of SA-

and contact angle with the size of the fluorinated silica nanoparticles in the film deposited on Al alloy substrate have also been discussed in the study of Brassard et al. [34]; where we have presented that the water contact angle as well as the surface roughness of the thin films increases with the increase of the size of the fluorinated silica nanoparticles.

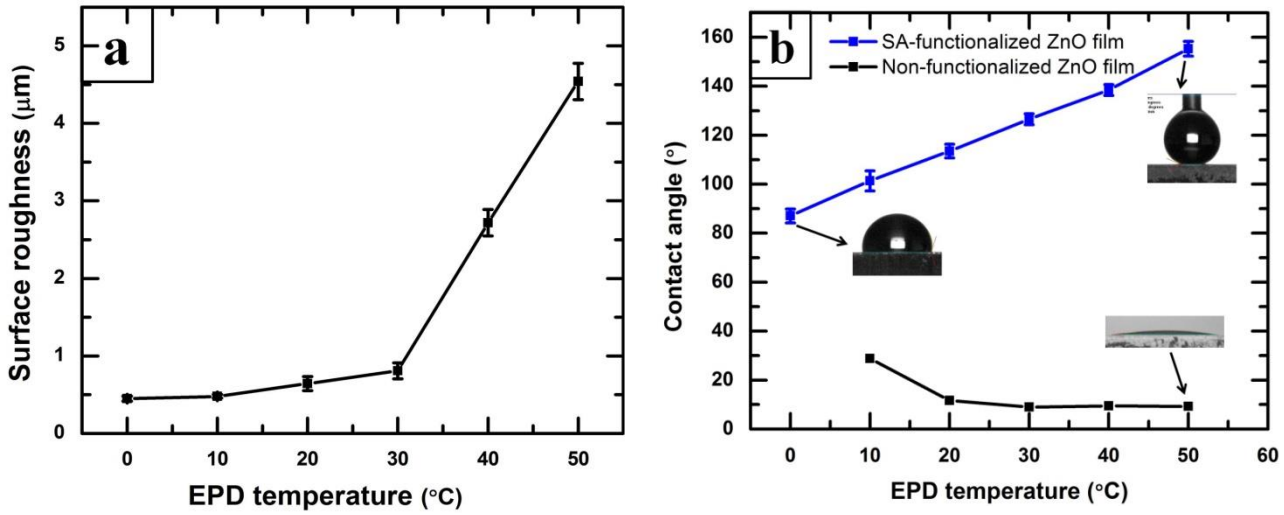

Figure 4(a) The variation of surface roughness thin films prepared from SA-functionalized ZnO nanoparticles at different bath temperature. (b) The variation of water contact angle of thin films prepared from (top) SA-functionalized ZnO nanoparticles (bottom) as received ZnO nanoparticles at different bath temperatures.

Fig. 5(a) compares energy dispersive x-ray microanalysis (EDX) spectra of SA-functionalized ZnO thin films deposited on aluminum alloy substrates at various bath temperature of the electrophoretic deposition (EPD) process. The peak Au M_{α} at 2.14 is observed, due to the thin layer of gold on the SA-functionalized ZnO thin films for improving the resolution by eliminating the charging effect of non-conducting samples during EDX analyses. The appearance of characterized

x-ray peaks of Zn L_α, K_α and K_β at 1.01 keV, 8.63 keV and 9.56 keV, respectively, confirms the presence of Zn. Similarly, the characteristics x-ray peak of O K_α at 0.52 keV is observed as the thin films composed of ZnO. This result is complementary with the analysis using XRD and FTIR as presented in Fig. 1(a) and (b). Fig. 5(a) also depicts that the intensity of the x-ray peaks of Zn as well as O increases with the increase of bath temperature. The atomic percentage of Zn has been calculated from the EDX data and presented in Fig. 5(b). It is found that the atomic percentage of Zn increases with the increase of bath temperature. It can be conferred from this results that the thickness of the SA-functionalized ZnO thin films also increases with the increase of bath temperatures. It can be seen in the Fig. 5(a) that the x-ray peak of Al K_α at 1.48 keV, coming for the aluminum alloy substrates, reduces drastically due to the enhance thickness of the SA-functionalized ZnO thin films grown at the bath temperature of 50°C. The results are also summarized in the Table 1.

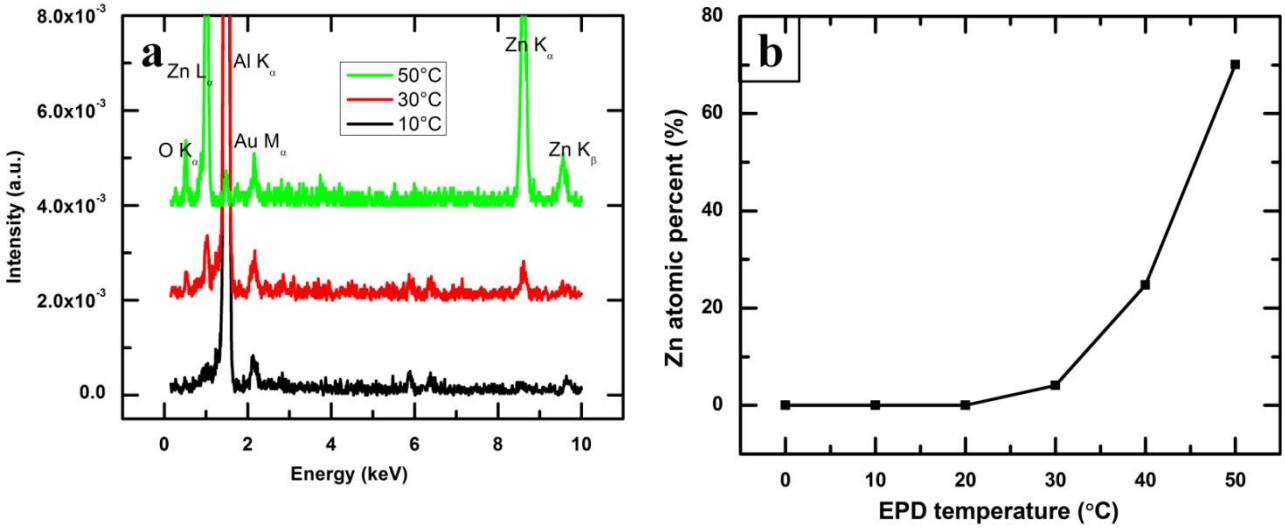

Figure 5(a) EDX spectra of SA-functionalized ZnO thin films as a function of bath temperature of EPD process; (b) Atomic percentage of Zn in the SA-functionalized ZnO thin films deposited at various bath temperature of EPD process as measured by EDX.

Fig. 6(a) shows the variation of the XRD peak area of ZnO (101) situated at 2θ of 36.2° for the thin films of SA-functionalized ZnO nanoparticles prepared by EPD process at varying bath temperature of 30-50 °C. The systematic increase of the XRD peak area indicates that the thickness of the deposited thin films of SA-functionalized ZnO nanoparticles increases with the increase of the bath temperature of the EPD process, which is complementary with the observation in the SEM images (Fig. 2(b-f)) as well as the EDX analyses in Fig. 5(b).

The colloidal nanoparticles in liquid suspension always undergo Brownian motion depending on their bath temperature. The constant thermal motion of the individual nanoparticles leads to collisions between them. The higher electrophoretic temperature, having a faster Brownian motion and collisions, decreases the sedimentation at the bottom of the bath due to the presence of less number of agglomerated particles. Therefore, more nanoparticles in suspension that enhances the deposition of nanoparticles on a substrate under the sufficient electric field [38].

Fig. 6(b) shows the variation of the logarithm of the XRD peak areas (A) as a function of the reciprocal of the bath temperatures (T). It is found that the logarithm of peak area decreases linearly as a function of the reciprocal of operating temperature (1/T), following the Arrhenius type of behavior as shown in Fig. 6(b) and presented in Eq. (2):

$$A = a_0 \exp\left(-\frac{E}{kT}\right) or\ \ln A = -\frac{E}{k}\left(\frac{1}{T}\right) - \ln(a_0) \quad (2)$$

where a_0 is a constant, E is the activation energy and k is the Boltzmann constant.

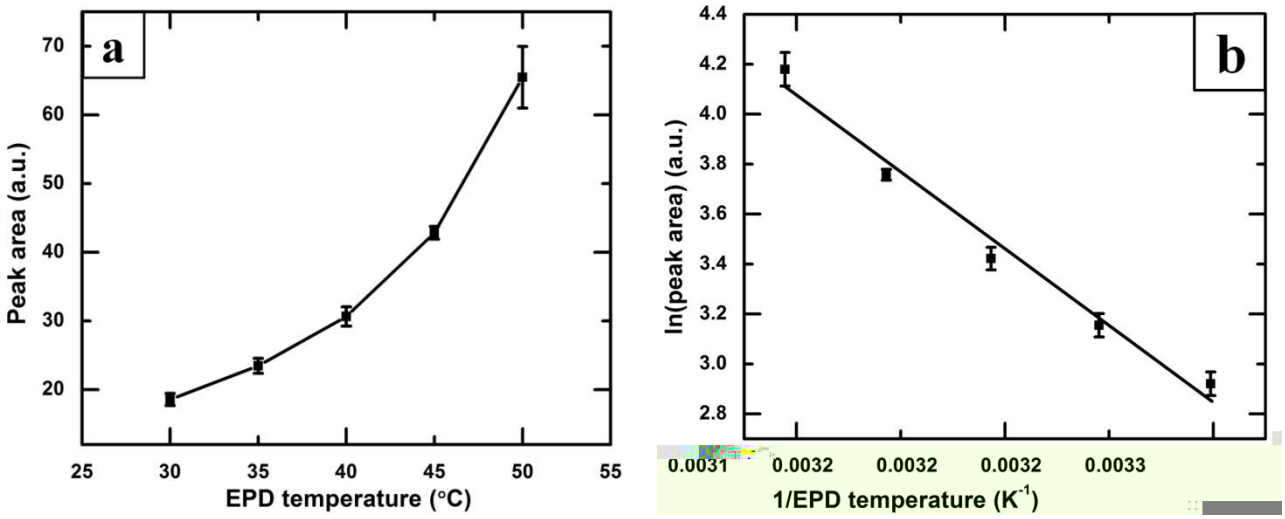

Figure 6(a) Variation of the area under the XRD peaks at 2θ of 36.19° of SA-functionalized ZnO thin films as a function of the EPD bath temperature. (b) Arrhenius plot of logarithm of the peak area vs. reciprocal of EPD temperature.

The activation energy for electrophoretic deposition of SA-functionalized ZnO nanoparticle is calculated to be 0.50 eV from Fig. 6(b). Saleema et al. [28] reported that the thermal desorption of stearic acid on superhydrophobic zinc oxide nanotowers on silicon substrates. The activation energy for desorption of SA from the ZnO surface is calculated to be 0.34 eV in the temperature range of 130-350 °C by those authors [28].

4. Conclusions

The one-step electrophoretic deposition (EPD) process has been developed to prepare superhydrophobic thin films on aluminum alloy substrates using stearic acid functionalized ZnO nanoparticles. The thickness of the thin films increased with the increase of the EPD bath temperature. XRD and FTIR studies confirmed the presence of stearic-acid-functionalized ZnO particles in the thin films. The surface morphology of the thin film shows large number of

micro-nanorough clusters of SA-functionalized ZnO nanoparticles and their intensity increases with the increase of bath temperatures. The water contact angle of 155 ± 3° with roll off property has been observed on the film that was grown at bath temperatures of 50 °C. Furthermore, the activation energy for electrophoretic deposition of SA-functionalized ZnO nanoparticle is calculated to be 0.50 eV.

Acknowledgements

We acknowledge the financial support provided by Natural Science and Engineering Research Council of Canada (NSERC), Aluminum Research Center (REGAL) and Centre Québécois de Recherche et de Développement de l'aluminium (CQRDA). We thank Dr. N. Saleema for acquiring the infrared data at the facilities of Aluminum Technology Centre, National Research Council of Canada (ATC-NRC), Saguenay.

References

[1] W. Barthlott, C. Neinhuis, Purity of the sacred lotus, or escape from contamination in biological surfaces, Planta, 202 (1997) 1-8.

[2] J.L. Gao X, Biophysics: water-repellent legs of water striders, Nature, 432 (2004) 36-.

[3] Y. Huang, D.K. Sarkar, X.G. Chen, A one-step process to engineer superhydrophobic copper surfaces, Mater. Lett. 64 (2010) 2722-2724.

[4] Y. Huang, D.K. Sarkar, X.G. Chen, Fabrication of superhydrophobic surfaces on aluminum alloy via electrodeposition of copper followed by electrochemical modification, Nano Micro lett. 3(3) (2011) 160-165.

[5] G.K. Paul, R. Ghosh, S.K. Bera, S. Bandyopadhyay, T. Sakurai, K. Akimoto, Deep level transient

spectroscopy of cyanide treated polycrystalline p-Cu2O/n-ZnO solar cell, Chem. Phys. Lett. 463 (2008) 117-120.

[6] K.V. Gurav, V.J. Fulari, U.M. Patil, C.D. Lokhande, O.-S. Joo, Room temperature soft chemical route for nanofibrous wurtzite ZnO thin film synthesis, Appl. Surf. Sci. 256 (2010) 2680-2685.

[7] J. Goldberger, D.J. Sirbuly, M. Law, P. Yang, ZnO Nanowire Transistors, J. Phys. Chem. B 109 (2004) 9-14.

[8] Z.D. Ding M., Yao B., E.S., Guo Z., Zhang L., Shen D., The ultraviolet laser from individual ZnO microwire with quadrate cross section, Opt. Express 20 (2012) 13657-13662.

[9] D. Basak, G. Amin, B. Mallik, G.K. Paul, S.K. Sen, Photoconductive UV detectors on sol–gel-synthesized ZnO films, J. Cryst. Growth 256 (2003) 73-77.

[10] M. Laurenti, V. Cauda, R. Gazia, M. Fontana, V.F. Rivera, S. Bianco, G. Canavese, Wettability Control on ZnO Nanowires Driven by Seed Layer Properties, Eur. J. Inorg. Chem. 2013 (2013) 2520-2527.

[11] A. Siddaramanna, N. Saleema, D.K. Sarkar, A versatile cost-effective and one step process to engineer ZnO superhydrophobic surfaces on Al substrate, Appl. Surf. Sci. 311 (2014) 182-188.

[12] J.Z. Mei Li, Huan Liu, Yanlin Song, Lei Jiang, and Daoben Zhu, Electrochemical Deposition of Conductive Superhydrophobic Zinc Oxide Thin Films, J. Phys. Chem. 107 (2003) 9954-9957.

[13] T.-C. Lee, W.-J. Wang, T.-Y. Han, Preparation of a Superhydrophobic ZnO Film on ITO Glass via Electrodeposition Followed by Oxidation. Effect of the Deposition Time, J. Adhes. Sci. Technol. 23 (2009) 1799-1810.

[14] N.L. Tarwal, P.S. Patil, Superhydrophobic and transparent ZnO thin films synthesized by spray pyrolysis technique, Appl. Surf. Sci. 256 (2010) 7451-7456.

[15] N.L. Tarwal, A.V. Rajgure, A.I. Inamdar, R.S. Devan, I.Y. Kim, S.S. Suryavanshi, Y.R. Ma, J.H. Kim,

P.S. Patil, Growth of multifunctional ZnO thin films by spray pyrolysis technique, Sensor Actuat. A-Phys. 199 (2013) 67-73.

[16] C. Mondal, M. Ganguly, A.K. Sinha, J. Pal, T. Pal, Fabrication of a ZnO nanocolumnar thin film on a glass slide and its reversible switching from a superhydrophobic to a superhydrophilic state, RSC Adv. 3 (2013) 5937.

[17] S. Yang, W. Cai, J. Yang, H. Zeng, General and Simple Route to Micro/Nanostructured Hollow-Sphere Arrays Based on Electrophoresis of Colloids Induced by Laser Ablation in Liquid, Langmuir, 25 (2009) 8287-8291.

[18] L. Besra, M. Liu, A review on fundamentals and applications of electrophoretic deposition (EPD), Prog. Mater Sci. 52 (2007) 1-61.

[19] Y.S. Joung, C.R. Buie, Electrophoretic Deposition of Unstable Colloidal Suspensions for Superhydrophobic Surfaces, Langmuir, 27 (2011) 4156-4163.

[20] H. Ogihara, T. Katayama, T. Saji, One-step electrophoretic deposition for the preparation of superhydrophobic silica particle/trimethylsiloxysilicate composite coatings, J. Colloid Interface Sci. 362 (2011) 560-566.

[21] H. Ogihara, J. Okagaki, T. Saji, A Facile Fabrication of Superhydrophobic Films by Electrophoretic Deposition of Hydrophobic Particles, Chem. Lett. 38 (2009) 132-133.

[22] Y. Huang, D.K. Sarkar, X.G. Chen, Preparation of nanostructured superhydrophobic copper and aluminum surfaces, in, Adv. Mater. Res. 2012, pp. 497-501.

[23] X.O. Yin, X.Z. Liu, L. Wang, B. Liu, Electrophoretic deposition of ZnO photoanode for plastic dye-sensitized solar cells, Electrochem. Commun. 12 (2010) 1241-1244.

[24] Y. Huang, D.K. Sarkar, D. Gallant, X.G. Chen, Corrosion resistance properties of superhydrophobic

copper surfaces fabricated by one-step electrochemical modification process, Appl. Surf. Sci. 282 (2013) 689-694.

[25] ZnO JCPDS # [00–003–0888].

[26] Al JCPDS # [01-085-1327].

[27] M.R. Mohammadi, F. Ordikhani, D.J. Fray, F. Khomamizadeh, Template-based growth of titanium dioxide nanorods by a particulate sol-electrophoretic deposition process, Particuology, 9 (2011) 161-169.

[28] N. Saleema, M. Farzaneh, Thermal effect on superhydrophobic performance of stearic acid modified ZnO nanotowers, Appl. Surf. Sci. 254 (2008) 2690-2695.

[29] H. Ogihara, J. Okagaki, T. Saji, Facile Fabrication of Colored Superhydrophobic Coatings by Spraying a Pigment Nanoparticle Suspension, Langmuir, 27 (2011) 9069-9072.

[30] H.W. Chen, C.Y. Lin, Y.H. Lai, J.G. Chen, C.C. Wang, C.W. Hu, C.Y. Hsu, R. Vittal, K.C. Ho, Electrophoretic deposition of ZnO film and its compression for a plastic based flexible dye-sensitized solar cell, J. Power Sources 196 (2011) 4859-4864.

[31] M. Verde, M. Peiteado, A.C. Caballero, M. Villegas, B. Ferrari, Electrophoretic Deposition of Transparent ZnO Thin Films from Highly Stabilized Colloidal Suspensions, J. Colloid Interface Sci. 373 (2012) 27-33.

[32] D.E.Rodak Y.T. Cheng, Turning the lotus effect on its head, Appl. Phys. Lett., 86 (2005) 144101.

[33] A.B.D. Cassie, Wettability of Porous Surfaces, Trans. Faraday Soc. 40 (1944) 546-551.

[34] J.D. Brassard, D.K. Sarkar, J. Perron, Synthesis of monodisperse fluorinated silica nanoparticles and their superhydrophobic thin films, **ACS** Appl. Mater. **Interfaces** 3 (2011) 3583.

[35] R. Wenzel, Resistance of solid surfaces to wetting by water, Ind. Eng. Chem. Res. 28 (1936) 988-994.

[36] Y.G. L. Xu, Q. Liao, J. Zhang, D. Xu, Morphological control of ZnO nanostructures by

electrodeposition, J. Phys. Chem. B 109 (2005) 13519-13522.

[37] C. Badre, T. Pauporté, M. Turmine, D. Lincot, A ZnO nanowire array film with stable highly water-repellent properties, Nanotechnology, 18 (2007) 365705.

[38] J.S. Gebauer, L. Treuel, Influence of individual ionic components on the agglomeration kinetics of silver nanoparticles, J. Colloid Interface Sci. 354 (2011) 546-554.